

AperTO - Archivio Istituzionale Open Access dell'Università di Torino

**Accumulation of sugars in the xylem apoplast observed under water stress conditions is controlled by xylem pH**

**This is the author's manuscript**

*Original Citation:*

*Availability:*

This version is available <http://hdl.handle.net/2318/1603307> since 2016-11-14T16:47:30Z

*Published version:*

DOI:10.1111/pce.12767

*Terms of use:*

Open Access

Anyone can freely access the full text of works made available as "Open Access". Works made available under a Creative Commons license can be used according to the terms and conditions of said license. Use of all other works requires consent of the right holder (author or publisher) if not exempted from copyright protection by the applicable law.

(Article begins on next page)

This is the author's final version of the contribution published as:

Secchi, Francesca; Zwieniecki, Maciej A.. Accumulation of sugars in the xylem apoplast observed under water stress conditions is controlled by xylem pH. *PLANT, CELL AND ENVIRONMENT*. 39 pp: 2350-2360.  
DOI: 10.1111/pce.12767

The publisher's version is available at:

<http://doi.wiley.com/10.1111/pce.12767>

When citing, please refer to the published version.

Link to this full text:

<http://hdl.handle.net/2318/1603307>

1 **Accumulation of sugars in the xylem apoplast observed under water stress conditions is**  
2 **controlled by xylem pH.**

3

4 **Short running title: Xylem pH regulates sugar accumulation in apoplast**

5

6 Francesca Secchi<sup>1</sup> and Maciej A. Zwieniecki<sup>2</sup>

7

8 <sup>1</sup>Department of Agricultural, Forest and Food Sciences (DISAFA), University of Torino, Italy

9 <sup>2</sup>Department of Plant Sciences, UC Davis, Davis, CA, USA

10

11 Corresponding author: Francesca Secchi

12 Department of Agricultural, Forest and Food Sciences (DISAFA), University of Torino, Largo

13 Paolo Braccini 2, 10095, Grugliasco (TO), Italy

14 Email: francesca.secchi@unito.it

15

16

17

18 **Abstract**

19 Severe water stress constrains, or even stops, water transport in the xylem due to embolism  
20 formation. Previously, the xylem of poplar trees was shown to respond to embolism formation  
21 by accumulating carbohydrates in the xylem apoplast and dropping xylem sap pH. We  
22 hypothesize that these two processes may be functionally linked as lower pH activates acidic  
23 invertases degrading sucrose and inducing accumulation of monosaccharides in xylem apoplast.  
24 Using a novel *in vivo* method to measure xylem apoplast pH, we show that pH drops from ~6.2  
25 to ~5.6 in stems of severely stressed plants and rises following recovery of stem water status.  
26 We also show that in a lower pH environment, sugars are continuously accumulating in the  
27 xylem apoplast. Apoplastic carbohydrate accumulation was reduced significantly in the presence  
28 of a proton pump blocker (orthovanadate). These observations suggest that a balance in sugar  
29 concentrations exists between the xylem apoplast and symplast that can be controlled by xylem  
30 pH and sugar concentration. We conclude that lower pH is related to loss of xylem transport  
31 function, eventually resulting in accumulation of sugars that primes stems for recovery from  
32 embolism when water stress is relieved.

33

34 **Keyword index:** *in vivo* pH, recovery, sugar accumulation, xylem apoplast

35

36

## 37 **Introduction**

38 Responding to continuous changes in soil water availability and atmospheric evaporative  
39 demand is a major part of plants' daily physiological activity. To ensure species survival in a  
40 given environment, a plant's transport system is expected to provide relatively uninterrupted  
41 supply of water for transpiration (Holbrook & Zwieniecki, 2008, Sperry, 2003, Sperry *et al.*,  
42 2003). However, long-lived trees may be exposed not only to these daily changes but also  
43 randomly occurring periods of severe drought that result in loss of xylem function (Holtta *et al.*,  
44 2009, Secchi & Zwieniecki, 2010, Tyree & Sperry, 1989, Zwieniecki & Holbrook, 2009). While  
45 recovery of xylem function may not be feasible under drought, increased water availability (rain,  
46 fog, snow etc.) followed by reduction in xylem tension may provide necessary stress relief to  
47 allow for restoration of xylem hydraulic capacity to pre-stress levels (Burgess & Dawson, 2004,  
48 Laur & Hacke, 2014, Mayr *et al.*, 2014).

49 Successful hydraulic recovery might depend on plant physiological activity during the onset of  
50 stress that 'primes' the stem for fast recovery under short-term temporary relief from severe  
51 stress. 'Hydraulic priming' might include biological activity of stem parenchyma cells that  
52 respond to loss of xylem transport function (i.e. cessation of transport) or direct presence of  
53 embolism (Brodersen & McElrone, 2013, Chitarra *et al.*, 2014, Nardini *et al.*, 2011, Salleo *et al.*,  
54 2004, Salleo *et al.*, 2009, Zwieniecki *et al.*, 2004). Recent studies describe changes in expression  
55 levels of genes in parenchyma cells responding to artificially induced embolism. Observed  
56 changes included up-regulation of carbohydrate metabolism enzymes (including the starch  
57 degradation pathway), sugar transporters, ion transporters and aquaporins (Secchi *et al.*, 2011,  
58 Secchi & Zwieniecki, 2010). Such a systemic response suggests physiological significance of the  
59 biological processes triggered by loss of xylem function.

60 Analysis of *Populus nigra* xylem sap chemistry associated with onset of water stress revealed  
61 specific changes in parenchyma cell physiological activity that dropped apoplastic pH and  
62 increased sugar concentration in the xylem sap (Secchi & Zwieniecki, 2012). Significant  
63 differences in pH were especially noticeable between sap collected from functional and non-  
64 functional vessels (the latter is presumed to be isolated from transpiration stream by embolism at  
65 distal location), showing values of pH ~6.5 and ~5.5 respectively. In addition to observed pH  
66 differences, sugar concentration in xylem sap collected from non-functional vessels was also  
67 significantly higher than in vessels that remained functional [(Secchi & Zwieniecki, 2012) and  
68 Fig. S1]. Although sugar concentrations could not generate pressure sufficient to counteract  
69 hydrostatic tension in the xylem and allow for xylem refilling under water stress ( $\Psi < -0.2$  MPa),  
70 they were within the range required for restoration of xylem function upon relief from water  
71 stress following re-watering of the trees ( $\Psi > -0.2$  MPa) (Secchi & Zwieniecki, 2012). Taken  
72 together, observed xylem sap chemistry and parenchyma cell gene expression support the  
73 hypothesis that increasing stress and loss of xylem transport result in parenchyma cell activities  
74 that prime stems for subsequent, fast recovery of xylem function upon plant rehydration to pre-  
75 stress levels.

76 Our recently proposed model provides a hypothetical explanation for the observed changes in  
77 xylem sap chemistry (please consult Secchi & Zwieniecki, 2012). Briefly, we first assume that  
78 water stress (i.e. embolism) increases the starch degradation rate (Salleo *et al.*, 2009) resulting in  
79 higher cellular sucrose concentration, a notion supported by the increased expression of enzymes  
80 from di-carbohydrate metabolic pathways that include starch degradation enzymes (Secchi *et al.*,  
81 2011). Increasing symplast sucrose concentration may shift the membrane sucrose gradient  
82 allowing for the sucrose efflux into apoplastic compartments via sucrose H-coupled transporters

83 as was recently shown experimentally (Geiger, 2011, Wippel *et al.*, 2010). Although most of the  
84 sucrose transporters have been characterized as H<sup>+</sup>-sugar importers, recently electrophysiological  
85 studies of sucrose-induced current of ZmSUT1 in oocytes revealed an alternative transport mode  
86 showing that this transporter can also mediate the active efflux of sucrose. The authors showed  
87 that ZmSUT1 protein catalyzed H<sup>+</sup>-coupled sucrose symport and that the transport depended on  
88 the direction of the sucrose and pH gradient as well as the membrane potential (Carpaneto *et al.*,  
89 2005, Carpaneto *et al.*, 2010). It is worthwhile to note, however, that the biochemical properties  
90 of plant sugar transporters have been studied in heterologous systems rather than in plants. In  
91 *planta*, transgenic potato plants with downregulated expression of StSUT1 showed a lower tuber  
92 yield when phloem unloading towards tubers was apoplastic, indicating a major role for StSUT1  
93 in efflux towards sink organs (Kuhn *et al.*, 2003). However, the proof of a dual mode of H<sup>+</sup>-  
94 sucrose transporters in living xylem parenchyma cells has to be clearly demonstrated yet.

95 As sucrose efflux is accompanied by proton efflux, apoplastic pH is expected to drop concurrent  
96 to rising sucrose concentration. A drop in pH from ~6.2 [a typical xylem sap operational value  
97 based on the average of 22 perennial species (Sharp & Davies, 2009) and poplar (Secchi &  
98 Zwieniecki, 2014)] to below 5.8 would result in an increase of apoplastic invertase (i.e. acidic  
99 invertase) activity. Invertase is responsible for hydrolyzing sucrose into glucose and fructose,  
100 thus promoting the reduction of the disaccharide concentration and at the same time increasing  
101 the production of the monosaccharides. This process would result in lower apoplast sucrose  
102 concentration, thus maintain the symplast-apoplast sucrose gradient that consequently would  
103 lead to a continuous sucrose efflux. However, a continuous drop of apoplastic pH would  
104 eventually slow the efflux as sucrose co-transporters are highly sensitive to the pH gradient  
105 (Bush, 1990, Carpaneto *et al.*, 2005, Geiger, 2011, Wippel *et al.*, 2010). Eventually, a new

106 homeostasis of pH and sucrose gradient between cells and apoplast would be achieved, where  
107 the sucrose gradient is maintained by apoplastic invertase activity and by the symplastic starch  
108 degradation rate. Further, the new pH gradient would be constrained by both proton efflux via  
109 sucrose transporters and influx of protons to the symplast via ion anti-porters and membrane  
110 proton pumps.

111 Here, we aim to directly test part of the above hypothesis-scenario that relates xylem  
112 apoplast pH to sugar accumulation. First, we provide direct evidence of xylem apoplast pH  
113 changes in response to water stress using a novel experimental setup that allows for *in vivo*  
114 determination of pH in tree stems. Further, we provide evidence from *in vitro* analysis of  
115 changes in sugar concentration in xylem sap in response to different apoplastic pH levels.

116

## 117 **Material and Methods**

### 118 *Plant materials*

119 Experiments were conducted on 1-year-old plants of hybrid white poplars (*Populus tremula* x  
120 *Populus alba*; Institut National de la Recherche Agronomique France clone 717-1B4). In total,  
121 28 poplars were used in two different experiments. Poplar were grown either two plants per 1L  
122 pot (*in vivo* experiment) or one plant in 4L pots (*in vitro* experiment) filled with potting mix.  
123 Plants were grown in a glasshouse with the following ambient conditions: temperature  
124 maintained in the range of 25–32°C and natural daylight supplemented with light from metal  
125 halogen lamps to maintain a minimum of 500–600  $\mu\text{mol photons m}^{-2} \text{ s}^{-1}$  during a 12-h-light/12-  
126 h-dark cycle. Plants were approximately 1.2-1.5 m tall at the onset of the two experiments:

127 (1) *In vivo* experiment aimed at analysis of pH changes in response to increasing water stress and  
128 recovery. Six plants were used in this study. Two plants were grown in one pot (1L size) under



129 no stress conditions (watered to field capacity every day) and then subjected to drought by  
130 withholding irrigation. Small pots allowed for induction of severe drought within 2-3 days. The  
131 duration of severe drought was limited to 24 hours and plants were then re-watered. During the  
132 entire time from stopping irrigation to final recovery, one plant in a pot (from two-plant system)  
133 was used to determine stem water potential (see methods below) while a different plant from the  
134 same pot was used to determine xylem apoplastic pH (see methods below). This procedure was  
135 utilized to avoid wounding of the plant that pH was measured on. Through the entire treatment  
136 from withholding irrigation, plants were kept in low-level light ( $\sim 200 \mu\text{mol m}^{-2} \text{s}^{-1}$  of PAR).

137 (2) *In vitro* experiment aimed to determine the kinetics of sugar efflux in response to different  
138 pH buffers. Twenty-two poplars were used in this study. Plants were never exposed to severe  
139 water stress.

140

#### 141 *Measurements of stem water potential*

142 Stem water potential was measured on non-transpiring leaves. Leaves were covered with  
143 aluminum foil and placed in a humidified plastic bag for at least 15 minutes prior to excision.  
144 After excision, leaves were allowed to equilibrate for an additional 20 minutes before the xylem  
145 pressure was measured using a Scholander-type pressure chamber (Soil Moisture Equipment  
146 Corp., Santa Barbara, CA, USA).

147

#### 148 *In vivo determination of xylem apoplast pH*

149 Xylem apoplast pH was determined using pH sensitive dye (carboxyfluorescein diacetate -  
150 CFDA) conjugated to 15 kD dextran. The 15 kD size dextran was used to provide assurance that  
151 dye would not be taken up by the living cells as the goal of the study was to determine xylem

152 apoplastic pH. CFDA was conjugated to dextran in the lab following the procedure described by  
153 de Belder and Granath (1973). CFDA dye provides a good estimate of pH for the range of 4 to 7  
154 determined as a ratio of fluorescence measured at 510 nm excited by 495 and 430 nm  
155 respectively (Geilfus & Muehling, 2011).

156 An 'in-lab' developed tool was built to determine fluorescence ratio (Fig. 1A). The system  
157 consisted of a sensor head attached to the plant with two fiber optics guides attached to it. One of  
158 the fiber optics was bifurcated with one end attached to a 430 nm light emitting diode (LED) and  
159 second end to a 495 nm LED, both narrow band ( $\pm 5$  nm). A second fiber optic cable collected  
160 reflected and fluorescent light and was linked to high gain photodiode via a narrow band 510 nm  
161 ( $\pm 2$  nm) filter (Fig. 1A). LEDs were controlled by a computer and turned on consecutively  
162 such that only one LED illuminated the stem at a time. Fluorescence was measured by a lock-in  
163 amplifier (International Light LI-1700) and data collected by a dedicated computer. To avoid  
164 photo bleaching of the dye in long-term experiments, we used low-level irradiance and  
165 controlled exposure time to few seconds measured once per hour.

166 Initial validation of system performance was done on micro-capillary tubes (5  $\mu$ L) filled  
167 with range of pH buffers (4.93 to 7.03 pH). Buffers were mixed with CFDA-dextran conjugate to  
168 a final concentration of 4 mg per mL of dye and fluorescence was measured (Fig. 1B.1). This  
169 test was followed by testing dye-dextran conjugate response to pH directly applied to poplar  
170 stems (Fig. 1B.2). Stems were prepared by removing a small section of bark with phloem (3x6  
171 mm) and exposing xylem (Fig 1A.1-3). The end of each stem section was connected via silicone  
172 tube to a manifold allowing for perfusion of a series of pH buffers (4.93-7.03) (Fig. 1A.5). Two  
173 techniques were tested (1) dye-dextran conjugate was applied directly to the xylem and (2) dye-  
174 dextran conjugate was soaked onto a small piece of filter paper (size of exposed xylem) that was

175 hydraulically connected to the xylem via 1.5% agarose gel (Fig. 1A.1-2). In both cases, the  
176 window in the bark was covered with a transparent plastic sheet sealed to the stem via silicone  
177 vacuum grease to remove the possibility of xylem surface drying (Fig. 1A.3). Final  
178 concentration of dye used in stem tests and all subsequent analysis was 20 mg of CFDA/Dextran  
179 conjugate per one gram of water. Large size (15kD) of the dye-dextran conjugates limited  
180 diffusion of the dye into the stem or from the filter paper to the stem while allowing for stem sap  
181 to diffuse freely.

182         Following the preparation procedure, pH buffers were consecutively perfused through the  
183 stems using low pressure (15kPa) and the fluorescence ratio measured on either soaked xylem or  
184 dye-soaked filter paper (Fig. 1B). The pH of the buffer perfused through the stem was  
185 determined and used in the calibration. In all cases a relatively good correlation between pH and  
186 a fluorescence ratio was observed, although ratios were specific to each stem (problem most  
187 likely related to uneven dye application or surface properties of observed field). This specificity  
188 resulted in the need of fluorescence/pH calibration for each stem following each *in vivo*  
189 measurement (Fig. 1B). In general, the filter paper approach produced a stronger fluorescence  
190 signal and a less variable calibration curve, although it also resulted in several minute delays in  
191 response time after switching of pH buffer when compared to the direct application of dye to the  
192 xylem. This delay was probably due to time required for buffer diffusion from xylem to filter  
193 paper through the agarose gel. As this delay was relatively short compared to the expected  
194 duration of experiment (minutes vs. hours), the 'filter paper' approach was selected for long-term  
195 experiments due to its stronger signal. Once placed on the stem, filter paper was not removed  
196 until conclusion of the experiment. Although signal strength was observed to diminish over time,  
197 it remained measurable up to 5 days (when test was stopped, it is possible that setup could be

198 used for even longer time). It is important to note that xylem window has to be perfectly sealed  
199 for gel junction to remain wet and thus provide the hydraulic connection between xylem and  
200 filter paper through entire experiment duration.

201 The calibration curve from the micro-capillary tubes could be fitted with a linear model (df=6,  
202  $R^2=0.976$ , SS=13.73) or a four-parameter sigmoid curve for the range from ~4.93 to ~7.03 pH  
203 (df=4,  $R^2=0.9991$ , SS=13.74), (Fig. 1B.1). An F-test ( $F=0.002$ ) did not suggest that the sigmoidal  
204 model provided a significantly better fit for a given pH range. Similarly, stem calibration curve  
205 could be fitted with linear model (df=6,  $R^2=0.993$ , SS=13.74) or four parameter sigmoidal model  
206 (df=4,  $R^2=0.996$ , SS=13.75), (Fig. 1B.3); again F-test ( $F=0.002$ ) did not suggest that sigmoidal  
207 model provided a significantly better fit for a given pH range. Thus, the linear model was used  
208 for the calibration line using two buffers (4.93 and 7.03) that were perfused through the stems of  
209 experimental plant at the conclusion of the stress experiment for 60 minutes each (allowing for  
210 equilibration time). Calibration was performed without touching the measuring setup. The stem  
211 was cut above and below the fluorescence measuring point and the upper end of the stem was  
212 connected via a silicone tube to a manifold (as done in the stem tests – see above).

213

#### 214 *In vitro experiments to determine kinetics of sugar efflux in response to apoplastic pH*

215 A total of 22 plants were selected. From each plant, six segments of branches with similar length  
216 and diameter were cut (length:  $76.75 \text{ mm} \pm 7.82$  and diameter:  $5.10 \text{ mm} \pm 0.77$ ). We removed  
217 0.8 cm of bark from both sides of the segment and wrapped entire segments with Parafilm sheets  
218 to avoid evaporation. An ‘in-lab’ sap perfusion tool was built to run the experiment (see Fig.  
219 1C). Both ends of the branch segments were fixed to silicone rubber tubing with volume of  
220 ~1mL (Fig. 1C.2). On one end tubes were closed, while on the other end tubes were connected to

221 a channel that allowed air pressure application (Fig. 1C.3). Tubes were filled with different  
222 buffer solutions or DI water (volume of 1 mL per stem). Once filled with the liquid, tubes were  
223 pressurized with 0.15 MPa for 15 sec every 90 sec to allow buffers to perfuse throughout the  
224 segments to the closed side and upon pressure release to return to the initial position. The  
225 perfusion system was submerged in water to prevent stem desiccation. At the pressurization site  
226 of the system each tube had an access channel allowing for the collection of the liquid sample  
227 from water being perfused through the stem segment. During the experiment 40  $\mu$ L of solution  
228 was collected from a single channel linked to individual segment after 10, 30, 60, 120 and 180  
229 minutes. The liquids collected were immediately stored at -80 °C.

230 To assess how pH influences the kinetics of sugar accumulation (exchange between  
231 xylem parenchyma and xylem sap), stem segments were subjected to four different treatments:

- 232 1- pH 4.5 buffer (100 ml of 0.1 M Potassium hydrogen phthalate, 17.4 ml of 0.1 M Sodium  
233 hydroxide, 82.6 ml of distilled water)
- 234 2- pH 6.5 buffer (100 ml of 0.1 M Potassium dihydrogen phosphate, 27.8 ml of 0.1 M  
235 Sodium hydroxide, 72.2 ml of distilled water)
- 236 3- DI water
- 237 4- DI water plus sodium orthovanadate, (BioLabs, New England, MA) used at concentration  
238 of 1.0 mM. Sodium orthovanadate is an inhibitor of many membrane P-type pumps,  
239 among which the plasmalemma proton pump.

240

241 *Soluble carbohydrate content and pH measurements in the efflux liquid in response to apoplastic*

242 *pH*

243 The anthrone-sulfuric acid assay (Leyva *et al.*, 2008) was used to quantify soluble carbohydrate  
244 content in the liquids. The anthrone reagent was prepared immediately before analysis by  
245 dissolving 0.1 g of anthrone (0.1%) in 100 mL of concentrated sulfuric acid (98%).  
246 Briefly, 150  $\mu$ l of anthrone reagent was added to each well of the microplate containing 50  $\mu$ L of  
247 standard solutions (see below), sample solutions and water. Plates were kept for 10 min at 4 °C.  
248 Then, plates were incubated 20 min at 100 °C. After heating, plates were cooled for 20 min at  
249 room temperature and absorbance at 620 nm was read with a microplate reader (Multiscan  
250 Thermo Scientific). Colorimetric response was compared to the glucose standard curve (0, 0.01,  
251 0.03, 0.1, and 0.3 g L<sup>-1</sup> glucose) and total carbohydrate content was calculated as mg/mL of  
252 glucose. Analysis of sugars using the anthrone method provided results similar to those obtained  
253 through the high-performance liquid chromatography (HPLC) technique, as shown in Fig. S2,  
254 and confirming the reliability of both methods. The pH of each sample was measured using a  
255 micro pH electrode (Thermo Scientific, Beverly, MA, USA).

256

#### 257 *Analyses of sucrose, glucose and fructose*

258 After thawing, the liquid samples were centrifuged at 15,000  $\times$  g for 10 min. The supernatant  
259 was filtered through a 0.2  $\mu$ m syringe filter (Millex-HP filter, Millipore Co., MA, USA) and  
260 collected in 1 ml glass vial and used for high-performance liquid chromatography (HPLC)  
261 analysis. Reverse phase-liquid chromatography (Agilent HPLC 1100 series, USA) was  
262 performed to determine individual sugar content (sucrose, glucose and fructose). Separation of  
263 sugars was performed with water as a mobile phase flowing at 0.6 ml min<sup>-1</sup> using an Aminex  
264 HPX-87C column (300 mm  $\times$  7.8 mm; Bio Rad Laboratories, Hercules, CA, USA), which was  
265 preceded by a micro-guard cartridge (Carbo-C, pH range 5–9, 30 mm  $\times$  4.6 mm; Bio Rad

266 Laboratories, Hercules, CA, USA) and maintained at 80 °C. A ten-microliter extract was injected  
267 by an auto-sampler and sugars were detected using a refractive index detector (Agilent G1362A).  
268 Chromatographic peaks were identified by comparing retention times with those of standards and  
269 by spiking samples with pure compounds while quantification was carried out using the external  
270 standard method. The concentrations of different sugars were expressed as mg/ml of fluid.

271

## 272 **Results**

273 *In vivo* determination of xylem pH using pH sensitive dye (carboxyfluorescein diacetate -  
274 CFDA) fused to 15kD dextran suggests that *Populus tremula* x *Populus alba* xylem operated at  
275 relatively constant value of pH (~ 6.2) across wide range of water stress levels. In poplars  
276 experiencing a severe drought (stem water potential below -2.5 MPa) a significant drop in xylem  
277 pH was observed (to the level of ~ 5.6), (Fig. 2B). The drop in pH coincided with turgor loss in  
278 leaves (Fig. 2A) and would coincide with significant loss of stem hydraulic conductivity with the  
279 percent loss of conductivity exceeding 80% for this level of stress (Secchi & Zwieniecki, 2014).  
280 Re-watering of the plants resulted in almost immediate (less than 2 hours) restoration of leaf  
281 turgor and in recovery of stem water potential to pre-stress values within 12 hours. Surprisingly,  
282 xylem pH lagged recovery of water potential for almost 24 hours before the pre-stress level of  
283 ~6.2 pH was reached (Fig. 2).

284 *In vitro* exposure of xylem to two levels of pH using buffers (4.5, 6.5) and to DI water  
285 resulted in significant changes of soluble sugar concentration in the liquid (Fig. 3). In all three  
286 treatments a fast increase in sugar content was observed over initial period of 10-20 minutes as  
287 both buffers and DI water applied were free of sugars (Fig. 3A). In the case of pH 6.5 buffer the  
288 sugar concentration plateaued very fast at the level of *c.* 0.2 mg/ml. Such plateauing was not

289 observed in the low pH 4.5 treatment over 3 hours of experiment duration; instead a continuous  
290 increase of sugar concentration was present reaching a content of 0.5 mg/ml at the end of the  
291 experiment (Fig. 3A). Acidity of the pH 6.5 buffer treatment stayed relatively constant over the  
292 duration of the experiment (~pH 6.2), while pH of the 4.5 buffer slowly rose, eventually reaching  
293 value of 5.15 pH (Fig. 3B). Estimate of the maximum pH from fitting available time trend data  
294 with the exponential rise to maximum function was ~5.6 pH (fitting statistics -  $R^2=0.95$ ,  
295  $p<0.001$ ); a value close to that observed in the *in vivo* pH determination (Fig. 2B). DI water  
296 treatment had relatively steady pH within the range of 7-7.5 (Fig. 3B) with sugar accumulation  
297 similar to that of ~6.5 pH buffer. The concentration of the sugars measured in the xylem at the  
298 end of each treatment was related to final pH values of the solution and the highest carbohydrate  
299 content was found at pH ~5 and low concentrations across the entire pH range from ~6.2 to 8.2  
300 (Fig. 4A). Rate of sugar accumulation during last hour of the *in vitro* experiment was near zero  
301 in the range of pH 6.2 to 8.2 and it was still strongly positive in pH c. 5-5.2 (Fig. 4B).

302         Analysis of the basic sugar composition (sucrose, glucose and fructose) in the perfused  
303 liquid revealed that in 4.5 pH treatment the sucrose concentration was very low (almost absent at  
304 the end of the treatment), while concentration of fructose and glucose was high and continuously  
305 increasing during the duration of the experiment (Fig. 5A-B). By the third hour of the experiment  
306 fructose and glucose were dominant sugars with similar concentrations (Fig.5A-B). In both 6.5  
307 pH buffer and DI water treatments sucrose was continuously present and its concentration was  
308 not rising in the third hour (there was no significant difference in sucrose content over the  
309 duration of the experiment), (Fig. 5C-E). Concentrations of glucose and fructose were also stable  
310 over this time period suggesting that the system reached equilibrium and no net carbohydrate  
311 efflux was present from parenchyma cells (Fig. 5D-F).



312 Sodium orthovanadate ( $\text{NaVO}_3$ ) treatment was applied to determine if plasma membrane  
313 proton pumps were directly involved in the recirculation of protons necessary to keep the pH  
314 gradient and to energize the sugar transporters. Unfortunately, the test only could be done in DI  
315 water as vanadate salt interacted with applied buffers and was previously shown to be unreliable  
316 in acidic environments (Vreugdenhil & Spanswick, 1987). In DI water, vanadate presence  
317 significantly reduced the apoplastic sugar accumulation. The efflux level was inhibited by 27%  
318 after only 10 minutes and maintained similar level of inhibition until the end of third hour with  
319 values ranging from 36 to 41% (Fig. 6A). The pH of the DI water and pH of  $\text{NaVO}_3$  solution  
320 changed in a similar manner over the duration of the experiment and was never different between  
321 two treatments at the same time (Fig. 6C). Thus, the observed reduction in sugar concentration  
322 can be linked directly to the presence of vanadate and its effect on proton availability for sucrose  
323 transporter activity (Fig. 6B).

324

## 325 **Discussion**

326 *In vivo* determination of xylem apoplast pH in *P. tremula x alba* in response to the onset of water  
327 stress reveals its relative homeostasis around a pH value of 6.2. This level was maintained until  
328 stem water potential reached -2.5 MPa. Continuous stress that resulted in leaf turgor loss  
329 coincided with a fast (~7 hours) drop of pH to a new level of ~5.6, which was later maintained  
330 despite a slower drop in stem water potential. As stress below -2.5 MPa was also shown to be  
331 correlated with >80% loss of conductivity in this species (Secchi & Zwieniecki, 2014), we  
332 suspect that the observed changes in pH might reflect a shift from mostly functional transpiring  
333 xylem (with active transpirational water stream) to mostly non-functional xylem (either  
334 embolized or hydraulically isolated from flow by embolism presence in distal locations, or xylem

335 characterized by loss of transpirational activity which would reflect leaf turgor loss and  
336 transpirational cessation due to stomatal closure). Plant rehydration did result in fast recovery of  
337 leaf turgor (2 hours) and stem water potential (12 hour) to pre-stress condition. However, xylem  
338 pH did not start to recover until 24 hours after the return of plant water potential to pre-stress  
339 conditions (36 hours after re-watering). The length of delay in recovery of pH is similar to the  
340 time necessary for the recovery of stem hydraulic function from severe stress as observed  
341 previously in this species [ $\sim$ 24 hours; (Secchi & Zwieniecki, 2014)], further supporting the  
342 notion that low pH in non-functional stem is linked to loss of transport function (Secchi &  
343 Zwieniecki, 2012).

344 Both sucrose concentration gradient and pH differences were previously shown to be  
345 associated with sucrose transporter activity, ultimately affecting both the direction and rate of  
346 sucrose transport (Carpaneto *et al.*, 2005, Wipfel *et al.*, 2010). Recently, a drop in xylem pH  
347 observed in non-functional vessels of poplar xylem (Secchi & Zwieniecki, 2012) was  
348 hypothesized to result from sucrose efflux occurring via sucrose/proton co-transporters. The  
349 lower pH has a positive effect on apoplastic invertase activity (Goetz & Roitsch, 1999) that  
350 effectively lowers apoplastic sucrose concentration, generating a sucrose concentration gradient  
351 that promotes sucrose efflux and accumulation of carbohydrates in xylem apoplast. The low  
352 apoplast pH effect on sugar accumulation in xylem apoplast is supported by our results where pH  
353 of  $\sim$ 4.5 led to continuous sugar accumulation in the xylem sap, mostly in the form of glucose and  
354 fructose (Fig. 3 and 5). We can further deduce that the efflux is mostly in the form of sucrose as  
355 higher pH (water and buffer) resulted in lower overall sugar concentration, but limited  
356 accumulation occurred in the form of sucrose (i.e. there was presumably very limited apoplastic  
357 invertase activity (Goetz & Roitsch, 1999). In addition, overall efflux was halted within 1 hour

358 in high pH, suggesting that the sucrose concentration gradient was a major driver of initial efflux  
359 activity (Fig. 3).

360 As efflux of sucrose from cells is coupled with co-transport of protons, a decrease in pH  
361 as observed in our experiments should be expected. However, this was not the case in both high  
362 and low pH treatments. In the high pH treatment, no significant changes in pH were observed  
363 over the duration of the experiment, while in the low pH treatment a significant increase of pH  
364 occurred (Fig. 3). Such behavior suggests that sucrose-coupled proton efflux is counter-balanced  
365 by increased proton pump activity. As the introduction of sodium orthovanadate (known proton  
366 pump blocker) significantly reduced sucrose efflux while not changing pH of the apoplast, we  
367 suspect that proton pumps not only work to maintain pH homeostasis (or return to pre-treatment  
368 state) but also might be involved in sucrose efflux control, a hypothesis also suggested by  
369 (Vreugdenhil & Spanswick, 1987) where vanadate inhibits the recycling of protons that were co-  
370 transported with sucrose. Such proton pump activity might be important for control of  
371 carbohydrate management under stress conditions. Results from the orthovanadate application  
372 have to be considered with caution as orthovanadate is a phosphate transition analog and  
373 therefore it could bind with (and block) any enzymatic process that depends on ATP hydrolysis.  
374 Thus, vanadate can probably be assumed to select for the H-ATPase only over periods of few  
375 minutes while during longer experiments it could affect all processes that depend on continuous  
376 turnover of ATP. However, even if only short time application is considered in our experiments  
377 (<10 minutes), the sugar efflux was already significantly reduced.

378 Taken together, our *in vivo* observations of pH changes under severe water stress conditions  
379 and the role of apoplastic pH in promoting sugar accumulation in the xylem support the  
380 hypothesis that apoplastic solute accumulation under stress conditions (Secchi & Zwieniecki,

381 2011) is ultimately controlled by xylem sap pH via acidic invertases and proton pump activity.  
382 While level of sugar accumulation may not allow for immediate recovery of xylem function  
383 under stress (Secchi & Zwieniecki, 2012), it could prime the xylem for accelerated restoration of  
384 xylem function upon return to hydrated conditions. We propose the following scenario of  
385 physiological events related to function of xylem parenchyma cells during onset of water stress  
386 and recovery (Fig. 7):

- 387 ○ Under normal hydration, xylem is functional and cells maintain near steady-state level of  
388 xylem sap pH. Such a situation continues even under moderate water stress, as suggested  
389 by our *in vivo* observation in conjunction with prior evidence that xylem sap pH changes  
390 in perennial plants experiencing stress which only partially closes stomata (Sharp &  
391 Davies, 2009). On average pH in such conditions is > 6, leading to very low invertases  
392 activity (Goetz & Roitsch, 1999), and sucrose flux direction is controlled by the low  
393 sucrose concentration in the cell due to higher starch accumulation, rather than pH (as  
394 high apoplastic pH promotes efflux).
- 395 ○ During severe water stress levels when embolism and/or stomatal closure occur, a plant  
396 would experience dramatic reduction in transpirational flow rates (Brodribb *et al.*, 2003,  
397 Buckley, 2005, Cochard *et al.*, 2002, McDowell *et al.*, 2008, Meinzer *et al.*, 2009,  
398 Nardini & Salleo, 2000, Urli *et al.*, 2013). This stop in transpirational flow would change  
399 the balance of carbohydrate fluxes in xylem, i.e. carbohydrates will not wash away in the  
400 transpiration stream, and the plant may experience temporary accumulation of sucrose in  
401 the apoplast that can trigger a cellular stress response promoting starch degradation  
402 (Secchi & Zwieniecki, 2011). Starch degradation results in increased cellular soluble  
403 sugar concentration (i.e. maltose and then sucrose), providing not only osmotic protection

404 from stress but also shifting the membrane sucrose gradient and triggering both passive  
405 (via membrane) and possibly proton-coupled sucrose efflux (Carpaneto *et al.*, 2005,  
406 Wipfel *et al.*, 2010) as treatment with sodium orthovanadate (proton transport blocker)  
407 seems to block this efflux. The proton coupled sucrose efflux might be responsible for  
408 initial increase of apoplastic sucrose concentration and drop of pH. Drop in pH could  
409 also be promoted by activity of H<sup>+</sup>-ATPase proton pumps.

410 ○ Lower pH leads to a several-fold increase in apoplastic invertase activity that splits  
411 sucrose to fructose and glucose and lowers sucrose concentration promoting its further  
412 efflux either via sucrose co-transporters or passive efflux through the membrane.  
413 Leveling of the apoplastic pH could be achieved by increased activity of ion anti-porters  
414 that would not only stabilize new lower pH but also increase metal ion concentration as  
415 previously seen (Secchi *et al.*, 2011, Secchi & Zwieniecki, 2012). This notion of pH  
416 stabilization is supported by our *in vivo* measurements where pH stabilized *c.* 5.6, and  
417 observed rise of pH in *in vitro* experiment (buffer 4.5 pH).

418 ○ Upon recovery from stress, sugars continuously accumulate in the xylem and pH remains  
419 low until full xylem functional recovery occurs. This recovery of transport function and  
420 the consequently removal of embolism is facilitated by both the high osmoticum level  
421 present in the xylem and whole plant level reduction of plant water stress (Secchi &  
422 Zwieniecki, 2012). As transpiration resumes, the cellular stress reaction is ‘triggered off’  
423 by washing away sugars and changing xylem pH as new water is delivered from roots.

424 In our proposed scenario, the recovery of stem functionality follows plant re-hydration,  
425 facilitated by a ‘priming’ of the xylem to recovery during stress via accumulation of solutes in  
426 the xylem apoplast.

427

428 **Acknowledgments**

429 F.S. acknowledges funding from ‘Programma Giovani Ricercatori Rita Levi Montalcini’ grant.

430 The authors wish to thank C. Crisosto and G. Hong for helping during the HPLC experimental

431 work. We would like to thank Mason Earls for editorial help with the manuscript.

432

433 **References**

434 Brodersen C.R. & McElrone A.J. (2013) Maintenance of xylem network transport capacity: a

435 review of embolism repair in vascular plants. *Frontiers in Plant Science*, **4**.

436 Brodribb T.J., Holbrook N.M., Edwards E.J. & Gutierrez M.V. (2003) Relations between

437 stomatal closure, leaf turgor and xylem vulnerability in eight tropical dry forest trees.

438 *Plant Cell and Environment*, **26**, 443-450.

439 Buckley T.N. (2005) The control of stomata by water balance. *New Phytologist*, **168**, 275-291.

440 Burgess S.S.O. & Dawson T.E. (2004) The contribution of fog to the water relations of *Sequoia*

441 *sempervirens* (D. Don): foliar uptake and prevention of dehydration. *Plant Cell and*

442 *Environment*, **27**, 1023-1034.

443 Bush D.R. (1990) Electrogenicity, pH-dependence and stoichiometry of the proton-sucrose

444 symport *Plant Physiology*, **93**, 1590-1596.

445 Carpaneto A., Geiger D., Bamberg E., Sauer N., Fromm J. & Hedrich R. (2005) Phloem-

446 localized, proton-coupled sucrose carrier ZmSUT1 mediates sucrose efflux under the

447 control of the sucrose gradient and the proton motive force. *Journal of Biological*

448 *Chemistry*, **280**, 21437-21443.

449 Carpaneto A., Koepsell H., Bamberg E., Hedrich R. & Geiger D. (2010) Sucrose- and H<sup>+</sup>-  
450 Dependent Charge Movements Associated with the Gating of Sucrose Transporter  
451 ZmSUT1. *Plos One*, **5**.

452 Chitarra W., Balestrini R., Vitali M., Pagliarani C., Perrone I., Schubert A. & Lovisolo C. (2014)  
453 Gene expression in vessel-associated cells upon xylem embolism repair in *Vitis vinifera*  
454 L. petioles. *Planta*, **239**, 887-899.

455 Cochard H., Coll L., Le Roux X. & Ameglio T. (2002) Unraveling the effects of plant hydraulics  
456 on stomatal closure during water stress in walnut. *Plant Physiology*, **128**, 282-290.

457 de Belder A.N. & Granath K. (1973) Preparation and properties of fluorescein-labelled dextrans.  
458 *Carbohydrate Research*, **30**, 375-378.

459 Geiger D. (2011) Plant Sucrose Transporters from a Biophysical Point of View. *Molecular Plant*,  
460 **4**, 395-406.

461 Geilfus C.-M. & Muehling K.H. (2011) Real-time imaging of leaf apoplastic pH dynamics in  
462 response to NaCl stress. *Frontiers in Plant Science*, **2**.

463 Goetz M. & Roitsch T. (1999) The different pH optima and substrate specificities of extracellular  
464 and vacuolar invertases from plants are determined by a single amino-acid substitution.  
465 *Plant Journal*, **20**, 707-711.

466 Holbrook N.M. & Zwieniecki M.A. (2008) Transporting water to the tops of trees. *Physics*  
467 *Today*, **61**, 76-77.

468 Holttä T., Cochard H., Nikinmaa E. & Mencuccini M. (2009) Capacitive effect of cavitation in  
469 xylem conduits: results from a dynamic model. *Plant Cell and Environment*, **32**, 10-21.

470 Kuhn C., Hajirezaei M.R., Fernie A.R., Roessner-Tunali U., Czechowski T., Hirner B. &  
471 Frommer W.B. (2003) The sucrose transporter StSUT1 localizes to sieve elements in

472 potato tuber phloem and influences tuber physiology and development. *Plant Physiology*,  
473 **131**, 102-113.

474 Laur J. & Hacke U.G. (2014) Exploring *Picea glauca* aquaporins in the context of needle water  
475 uptake and xylem refilling. *New Phytologist*, **203**, 388-400.

476 Leyva A., Quintana A., Sanchez M., Rodriguez E.N., Cremata J. & Sanchez J.C. (2008) Rapid  
477 and sensitive anthrone-sulfuric acid assay in microplate format to quantify carbohydrate  
478 in biopharmaceutical products: Method development and validation. *Biologicals*, **36**, 134-  
479 141.

480 Mayr S., Schmid P., Laur J., Rosner S., Charra-Vaskou K., Daemon B. & Hacke U.G. (2014)  
481 Uptake of water via branches helps timberline conifers refill embolized xylem in late  
482 winter. *Plant Physiology*, **164**, 1731-1740.

483 McDowell N., Pockman W.T., Allen C.D., Breshears D.D., Cobb N., Kolb T., Plaut J., Sperry J.,  
484 West A., Williams D.G. & Yezzer E.A. (2008) Mechanisms of plant survival and  
485 mortality during drought: why do some plants survive while others succumb to drought?  
486 *New Phytologist*, **178**, 719-739.

487 Meinzer F.C., Johnson D.M., Lachenbruch B., McCulloh K.A. & Woodruff D.R. (2009) Xylem  
488 hydraulic safety margins in woody plants: coordination of stomatal control of xylem  
489 tension with hydraulic capacitance. *Functional Ecology*, **23**, 922-930.

490 Nardini A., Lo Gullo M.A. & Salleo S. (2011) Refilling embolized xylem conduits: Is it a matter  
491 of phloem unloading? *Plant Science*, **180**, 604-611.

492 Nardini A. & Salleo S. (2000) Limitation of stomatal conductance by hydraulic traits: sensing or  
493 preventing xylem cavitation? *Trees-Structure and Function*, **15**, 14-24.



494 Salleo S., Lo Gullo M.A., Trifilo' P. & Nardini A. (2004) New evidence for a role of vessel-  
495 associated cells and phloem in the rapid xylem refilling of cavitated stems of *Laurus*  
496 *nobilis* L. *Plant, Cell and Environment*, **27**, 1065-1076.

497 Salleo S., Trifilo' P., Esposito S., Nardini A. & Lo Gullo M.A. (2009) Starch-to-sugar conversion  
498 in wood parenchyma of field-growing *Laurus nobilis* plants: a component of the signal  
499 pathway for embolism repair? *Functional Plant Biology*, **36**, 815-825.

500 Secchi F., Gilbert M.E. & Zwieniecki M.A. (2011) Transcriptome response to embolism  
501 formation in stems of *Populus trichocarpa* provides insight into signaling and the biology  
502 of refilling. *Plant Physiology*, **157**, 1419-1429.

503 Secchi F. & Zwieniecki M.A. (2010) Patterns of PIP gene expression in *Populus trichocarpa*  
504 during recovery from xylem embolism suggest a major role for the PIP1 aquaporin  
505 subfamily as moderators of refilling process. *Plant, Cell and Environment*, **33**, 1285-  
506 1297.

507 Secchi F. & Zwieniecki M.A. (2011) Sensing embolism in xylem vessels: the role of sucrose as a  
508 trigger for refilling. *Plant, Cell and Environment*, **34**, 514-524.

509 Secchi F. & Zwieniecki M.A. (2012) Analysis of Xylem Sap from Functional (Nonembolized)  
510 and Nonfunctional (Embolized) Vessels of *Populus nigra*: Chemistry of Refilling. *Plant*  
511 *Physiology*, **160**, 955-964.

512 Secchi F. & Zwieniecki M.A. (2014) Down-Regulation of Plasma Intrinsic Protein1 Aquaporin  
513 in Poplar Trees Is Detrimental to Recovery from Embolism. *Plant Physiology*, **164**, 1789-  
514 1799.

515 Sharp R.G. & Davies W.J. (2009) Variability among species in the apoplastic pH signalling  
516 response to drying soils. *Journal of Experimental Botany*, **60**, 4361-4370.

517 Sperry J.S. (2003) Evolution of water transport and xylem structure. *International Journal of*  
518 *Plant Sciences*, **164**, S115-S127.

519 Sperry J.S., Stiller V. & Hacke U.G. (2003) Xylem hydraulics and the soil-plant-atmosphere  
520 continuum: Opportunities and unresolved issues. *Agronomy Journal*, **95**, 1362-1370.

521 Tyree M.T. & Sperry J.S. (1989) Vulnerability of xylem to cavitation and embolism. *Annual*  
522 *Reviews of Plant Physiology and Molecular Biology*, **40**, 19-38.

523 Urli M., Porte A.J., Cochard H., Guengant Y., Burllett R. & Delzon S. (2013) Xylem embolism  
524 threshold for catastrophic hydraulic failure in angiosperm trees. *Tree Physiology*, **33**,  
525 672-683.

526 Vreugdenhil D. & Spanswick R.M. (1987) The effect of vanadate on proton-sucrose cotransport  
527 in *Ricinus* cotyledons. *Plant Physiology*, **84**, 605-608.

528 Wipfel K., Wittek A., Hedrich R. & Sauer N. (2010) Inverse pH Regulation of Plant and Fungal  
529 Sucrose Transporters: A Mechanism to Regulate Competition for Sucrose at the  
530 Host/Pathogen Interface? *Plos One*, **5**.

531 Zwieniecki M.A. & Holbrook N.M. (2009) Confronting Maxwell's demon: biophysics of xylem  
532 embolism repair. *Trends in Plant Science*, **14**, 530-534.

533 Zwieniecki M.A., Melcher P.J., Feild T. & Holbrook N.M. (2004) A potential role for xylem-  
534 phloem interactions in the hydraulic architecture of trees: effects of phloem girdling on  
535 xylem hydraulic conductance. *Tree Physiology*, **24**, 911-917.

536

537

538

539 **Figure legends**

540 **Figure 1**

541 **(A)** Preparation of stem for *in vivo* pH measurements. (A1) A small section of bark and phloem  
542 is removed (~3x6 mm). (A2) Exposed xylem is immediately covered with filter paper of the  
543 same size as the exposed xylem. Filter paper is pre-soaked with CFDA-dextran conjugate (at a  
544 concentration of 20 mg/g of water) and 1.5% agarose gel. Thick layer of vacuum grease (Dow  
545 Corning) is smeared on the bark around the filter paper. (A3) A transparent plastic sheet is  
546 placed over the filter paper and sealed to stem via vacuum grease protecting filter paper from  
547 drying out. (A4) Prepared section of the stem is then covered with perfectly light-tight clip with  
548 both bifurcated fiber optic guide connected to two narrow band light emitting diodes (LED;  
549 wavelength 495 and 430 nm +/-5 nm) and separate optic guide linked to high sensitivity high  
550 gain photodiode (International Light) connected. Fiber optics ends are placed over the filter  
551 paper. LEDs are consecutively turned on for six seconds once every hour and the fluorescence  
552 measured using narrow band light filter (510 nm +/-2). Measurements were conducted over 100  
553 hours without any alteration to the system. (A5) At the conclusion of the experiment, the stem  
554 was cut above and below the fiber optics attachment (without any disturbance to the setup) and a  
555 plastic tube was attached to upper part of the stem. Then two pH buffers (4.93 and 7.03) were  
556 perfused consecutively through the stem for 60 minutes each and fluorescence measurements  
557 performed to allow for stem-specific calibration. **(B)** Three calibration approaches are presented  
558 for the use of the pH sensitive dye (CFDA) conjugated to 15 kD dextran. (B1): Test of solution  
559 in capillary tube. Capillary tubes (5 µL) were filled with buffers of specific pH (4.93, 5.34, 5.66,  
560 6.03, 6.21, 6.48, 6.79, and 7.03) mixed with CFDA-dextran conjugate (at a final concentration of  
561 4 mg/g of water), sealed at both ends, and measured. (B2): Test on branch segment with exposed

562 xylem. In this experiment dye soaked directly to exposed xylem. (B3): Test on branch segment  
563 with exposed xylem. Dye soaked to filter paper fused to exposed xylem via 1.5% agarose gel on  
564 a 5 cm long stem segment. For approach B2) and B3) stem segments were consecutively  
565 perfused with pH buffers (4.93, 5.34, 5.66, 6.03, 6.21, 6.48, 6.79, and 7.03) prior to  
566 measurements. Dye on exposed xylem B(2) produced highly variable outcome, while filter paper  
567 approach B(3) resulted in strong signal to noise ratio and well-defined calibration curve for each  
568 stem (dotted lines represent sigmoidal four parameter fit and continuous lines represents two-  
569 parameter linear fit (see methods for statistical analysis)). (C) An ‘in-lab’ sap perfusion tool was  
570 built to determine the kinetics of sugar efflux in response to apoplastic pH. Around 7.5 cm long  
571 stem segments (C1) were connected via silicon rubber tubes (C2) to manifold (C3). Manifold on  
572 the right provided a cup to each stem while on the left it was consecutively pressurized and de-  
573 pressurized forcing liquid to flow back and forth through the stem. A glass capillary (C4) was  
574 used to collect sample of liquid being perfused through each stalk.

575

## 576 **Figure 2**

577 *In vivo* determination of xylem pH changes in response to water stress.

578 (A) Leaf turgor dynamics during increase in and recovery from water stress. (B) Xylem pH and  
579 stem water potential are plotted over the time. Blue arrow indicates the time of the addition of  
580 water (recovery). Black arrows represent the status of leaf turgor at the determined time.

581

## 582 **Figure 3**

583 Temporal changes of (A) nonstructural carbohydrate concentrations and (B) pH values in  
584 segments of stems incubated in pH 4.5- pH 6.5 buffers and in DI water for 3 hours.

585 One-way Anova tests suggest significant differences among the three buffer treatments and  
586 among the times of incubation for each treatment ( $p < 0.05$ ). Letters denote homogeneous groups  
587 based on the Fisher LSD method (lower-case letter, differences among treatments; upper-case  
588 letter, differences among times for the same treatment). Data are mean values and bars are SE.

589

#### 590 **Figure 4**

591 **(A)** Final sugar concentration as a function of pH value measured at the end of the treatments.  
592 Inset: Average xylem sugar content measured at the end of each treatment as it relates to final pH  
593 values. **(B)** Final rate of nonstructural carbohydrate accumulation as a function of pH value  
594 measured at the end of the treatments. Inset: Average sugar accumulation rate as it relates to final  
595 pH. For both insets, one-way Anova tests suggest significant differences between treatments ( $P$   
596  $< 0.01$ ). Letters denote homogeneous groups based on Fisher LSD method. Data are mean values  
597 and bars are SE.

598

#### 599 **Figure 5**

600 Sucrose, glucose and fructose content in portions of stems incubated for 3 hours in pH 4.5, pH 6.5  
601 buffers and DI water. Data are mean values and bars are SE. Statistical analysis has been done for  
602 each sugar independently and the Anova analysis reveals the presence of significant differences  
603 ( $p < 0.05$ ) among times. Letters denote homogeneous groups based on the Fisher LSD test.

604

#### 605 **Figure 6**

606 Effect of sodium orthovanadate on nonstructural carbohydrate content expressed as **(A)** percent of  
607 inhibition; no differences are observed among different times of the treatment (Anova analysis,

608  $p=0.311$ ) instead the percent of vanadate inhibition is different to zero (t-test, \*\*\*,  $p<0.001$ ), and  
609 as **(B)** concentration. Presence of orthovanadate significantly reduced sugar accumulation in  
610 xylem sap in each time of the treatment when compared with samples treated with water (paired t-  
611 test, \*,  $p<0.05$ ) while there was no significant effect of time on sugar accumulation in water (one-  
612 way Anova  $p=0.30$ ) and in orthovanadate treatment (one-way Anova,  $p=0.22$ ).

613 **(C)** Effect of vanadate on buffer pH. No differences are found between the two treatments; pH  
614 values do not change over the incubation period with vanadate while a one-way Anova test  
615 suggests differences between pH values for DI water over the time ( $p<0.05$ ). Letters denote  
616 homogeneous groups based on Fisher LSD test (lower-case letter, differences between the two  
617 treatments; upper-case letter, differences among times). Data are mean values and bars are SE.  
618 Orthovanadate concentration used was 0.1mM which was added at time = 0 of the incubation.

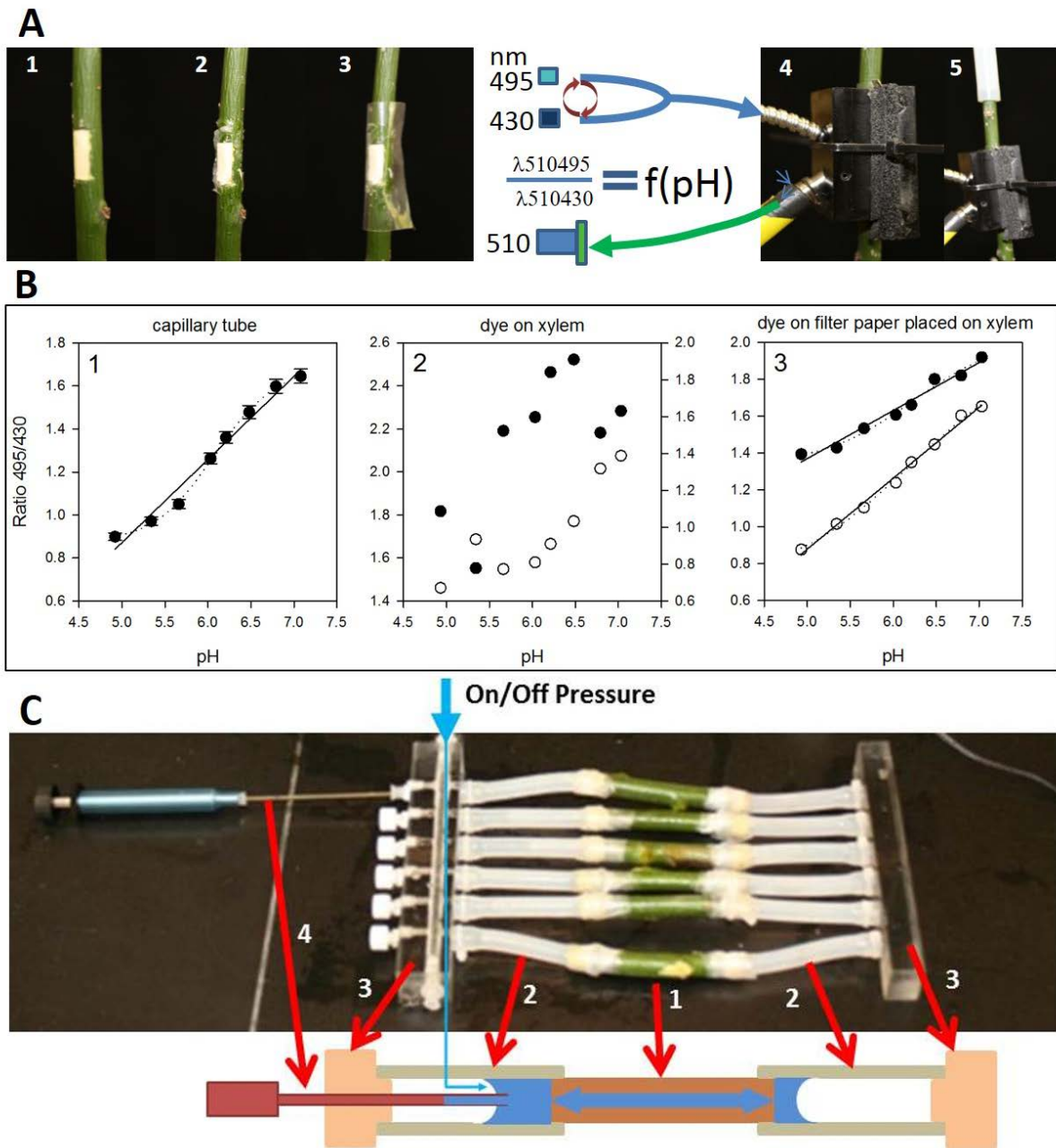
619

## 620 **Figure 7**

621 Schematic illustration of proposed membrane transporter activity during onset of stress and  
622 recovery from stress. Results from former studies (Secchi et al., 2011, Secchi & Zwieniecki,  
623 2012) are denoted as gray scale part of the figure. New aspect of related to the role of pH on the  
624 efflux of sugars to apoplast studied in this work is denoted by blue arrows and red text. For  
625 details of overall of scenario describing stem parenchyma cell activity, please refer to the text.

626

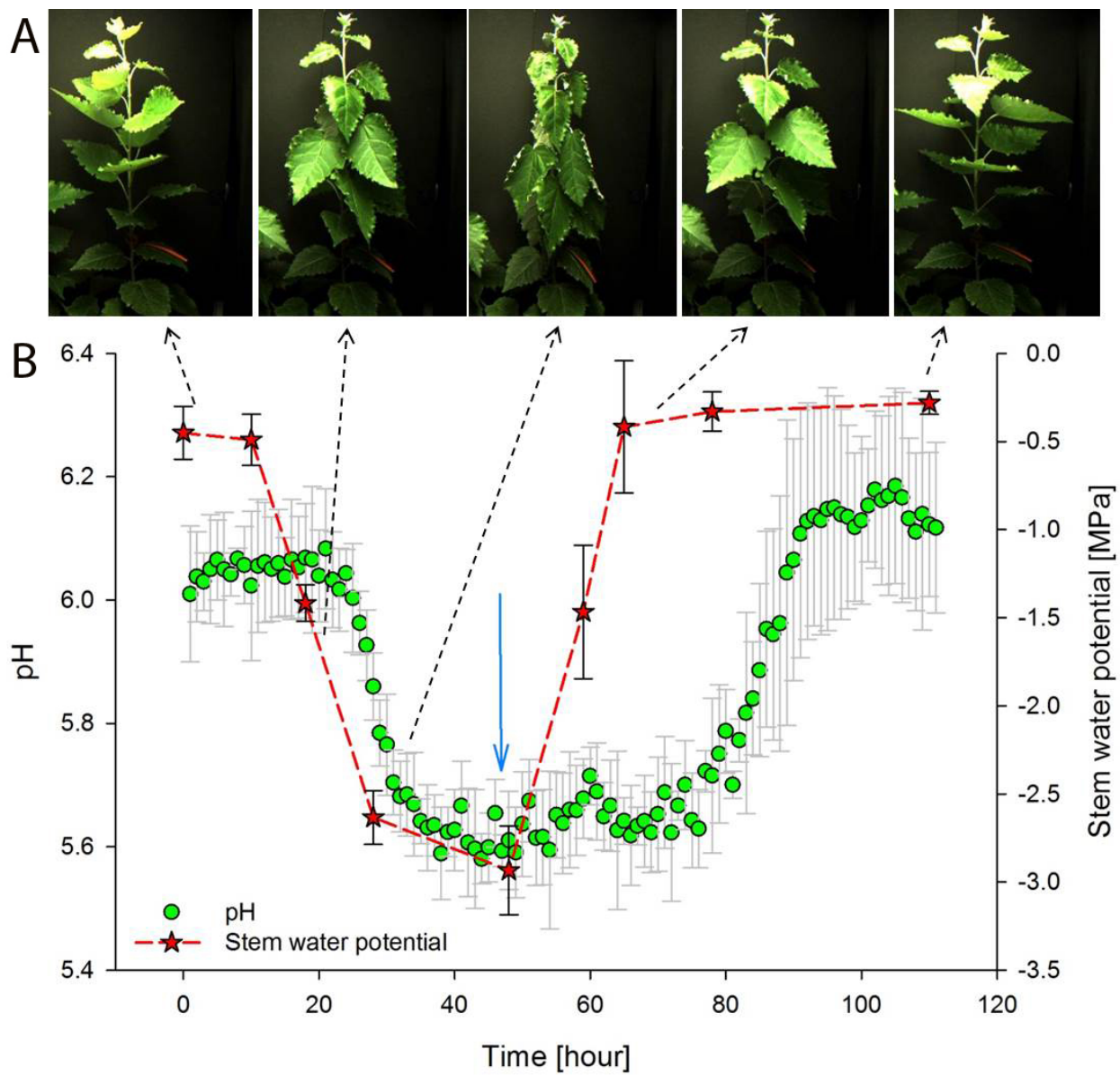
627 **Figure 1**



628

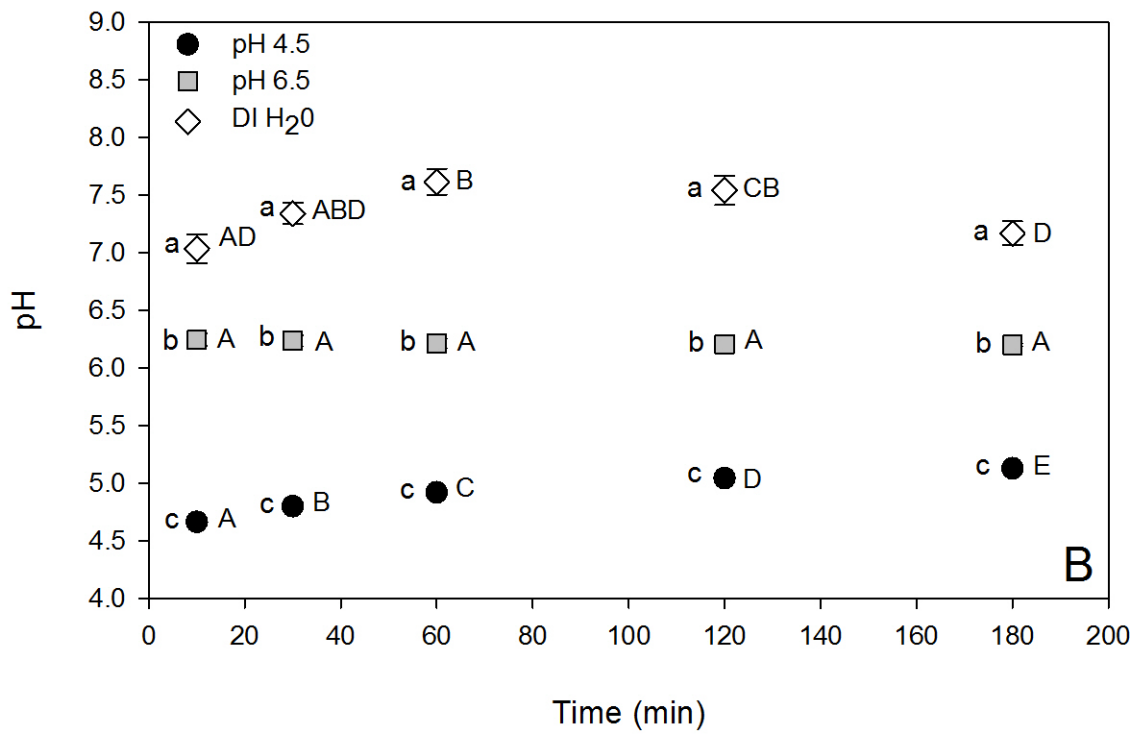
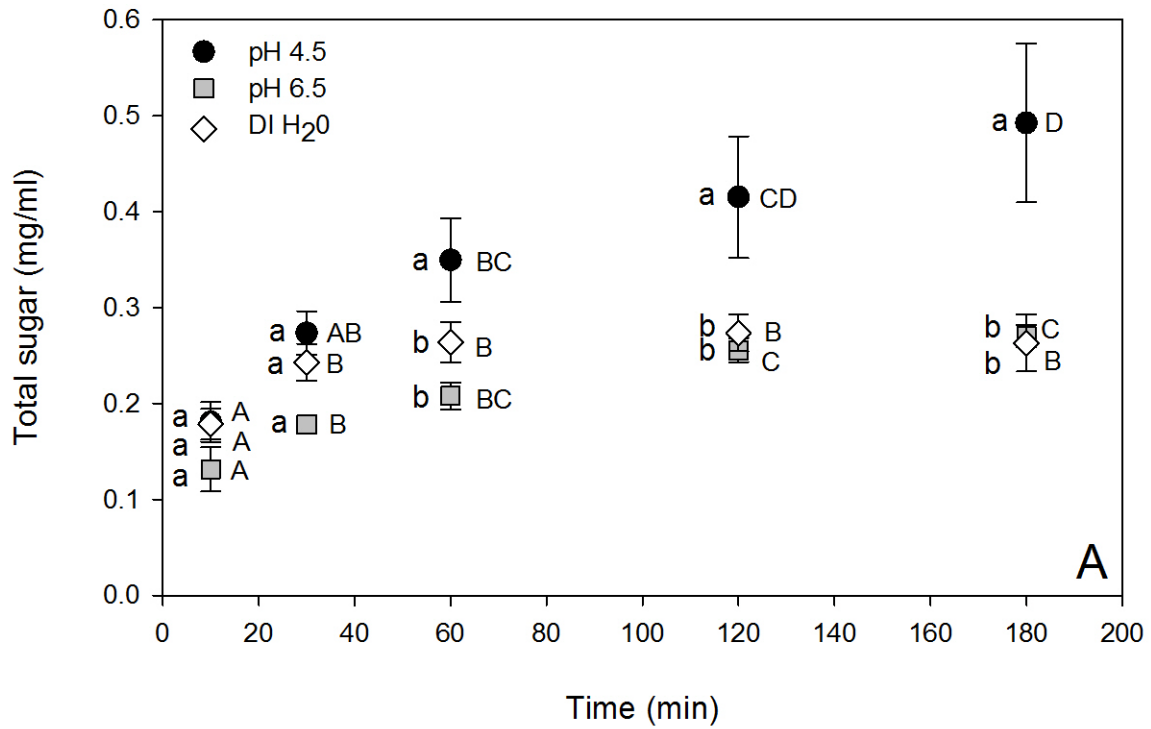
629

630 **Figure 2**  
631





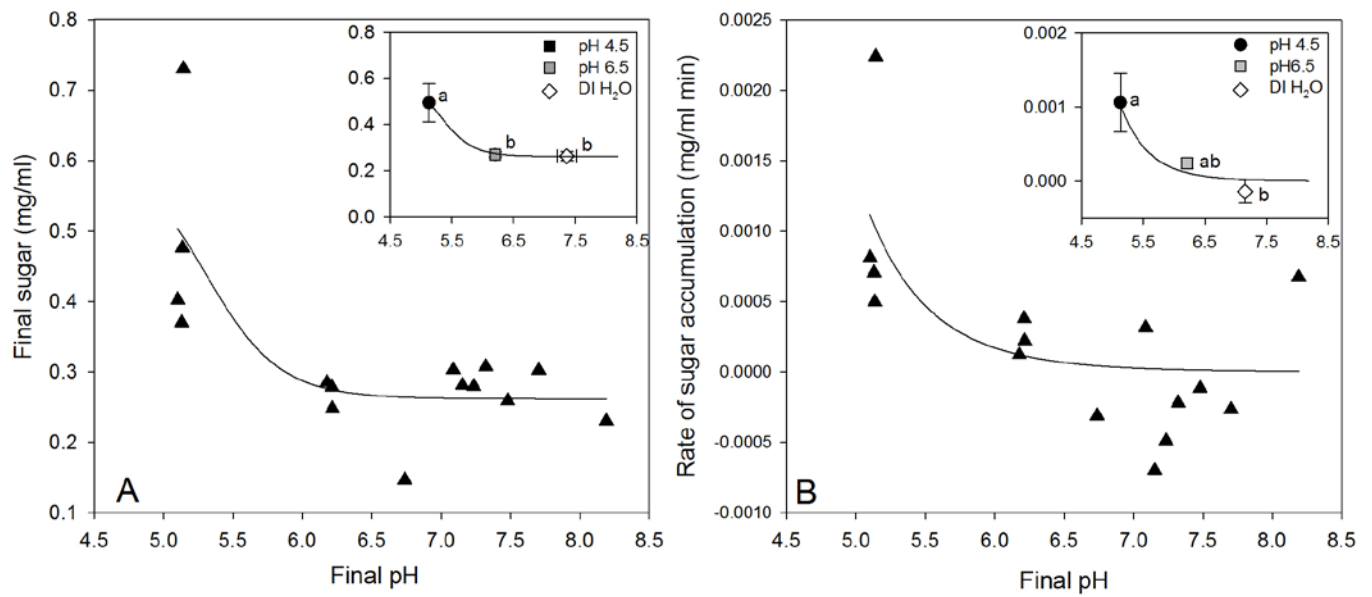
634 **Figure 3**



635

636

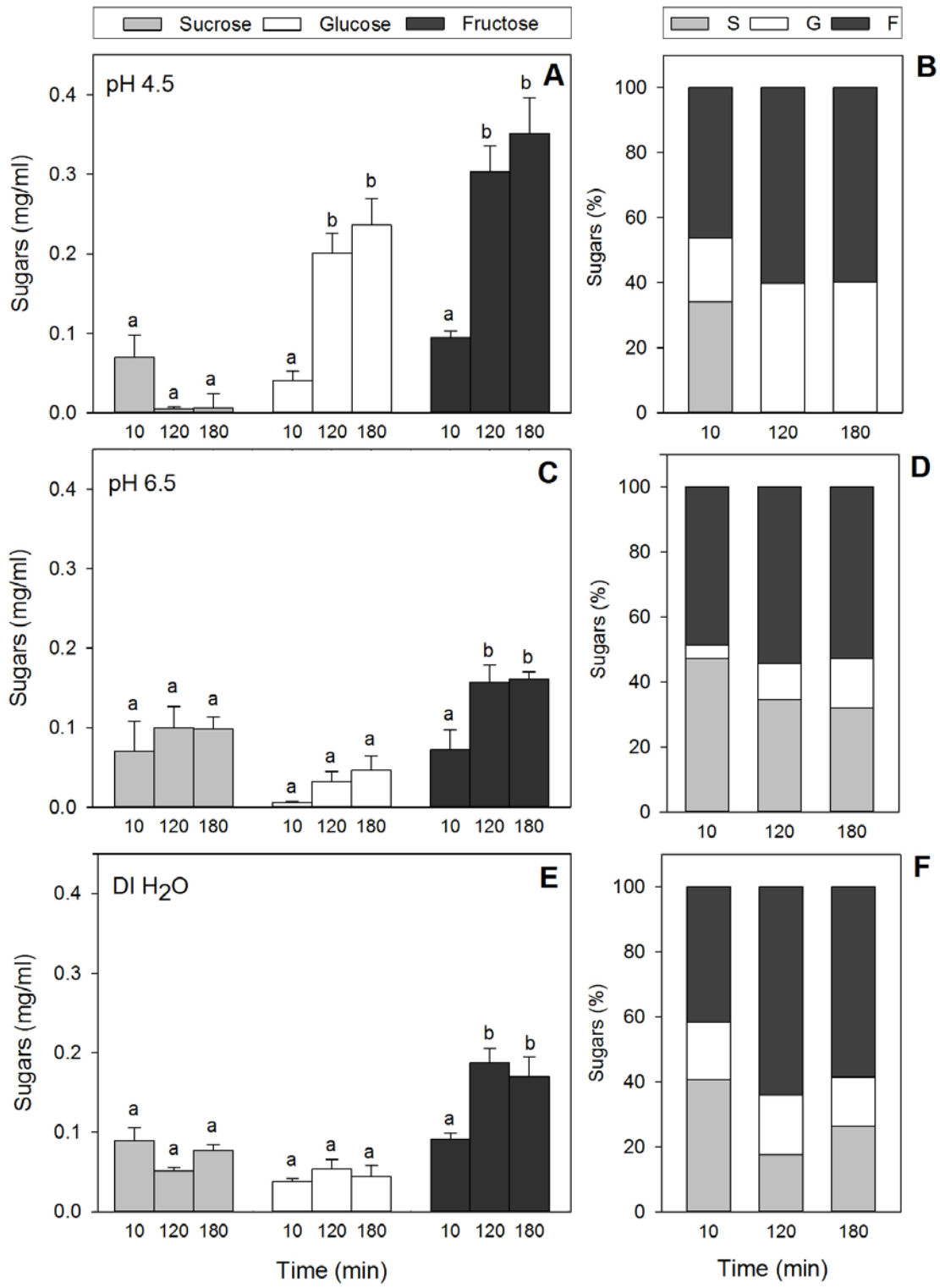
637 **Figure 4**



638

639

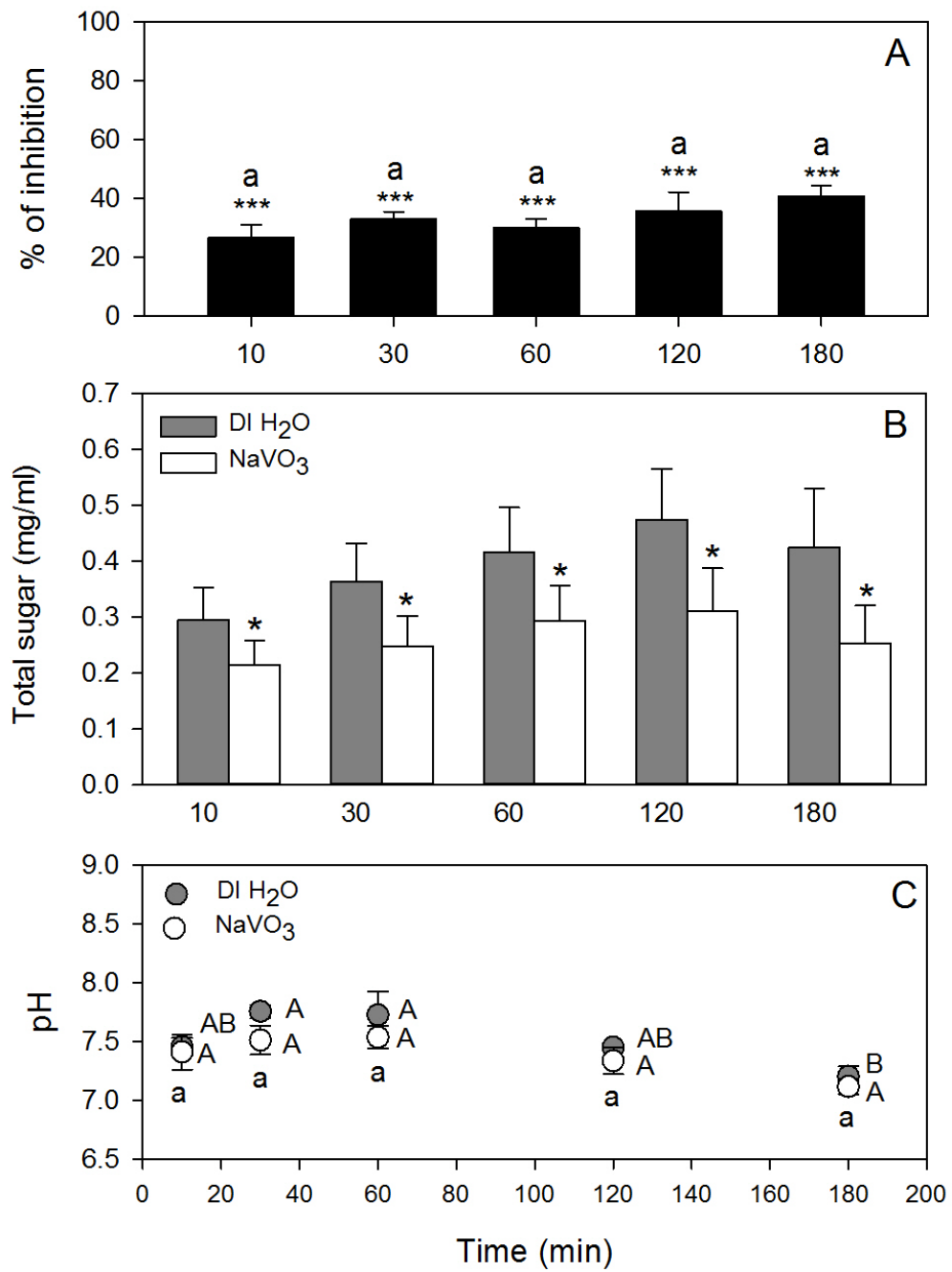
640 **Figure 5**



641

642

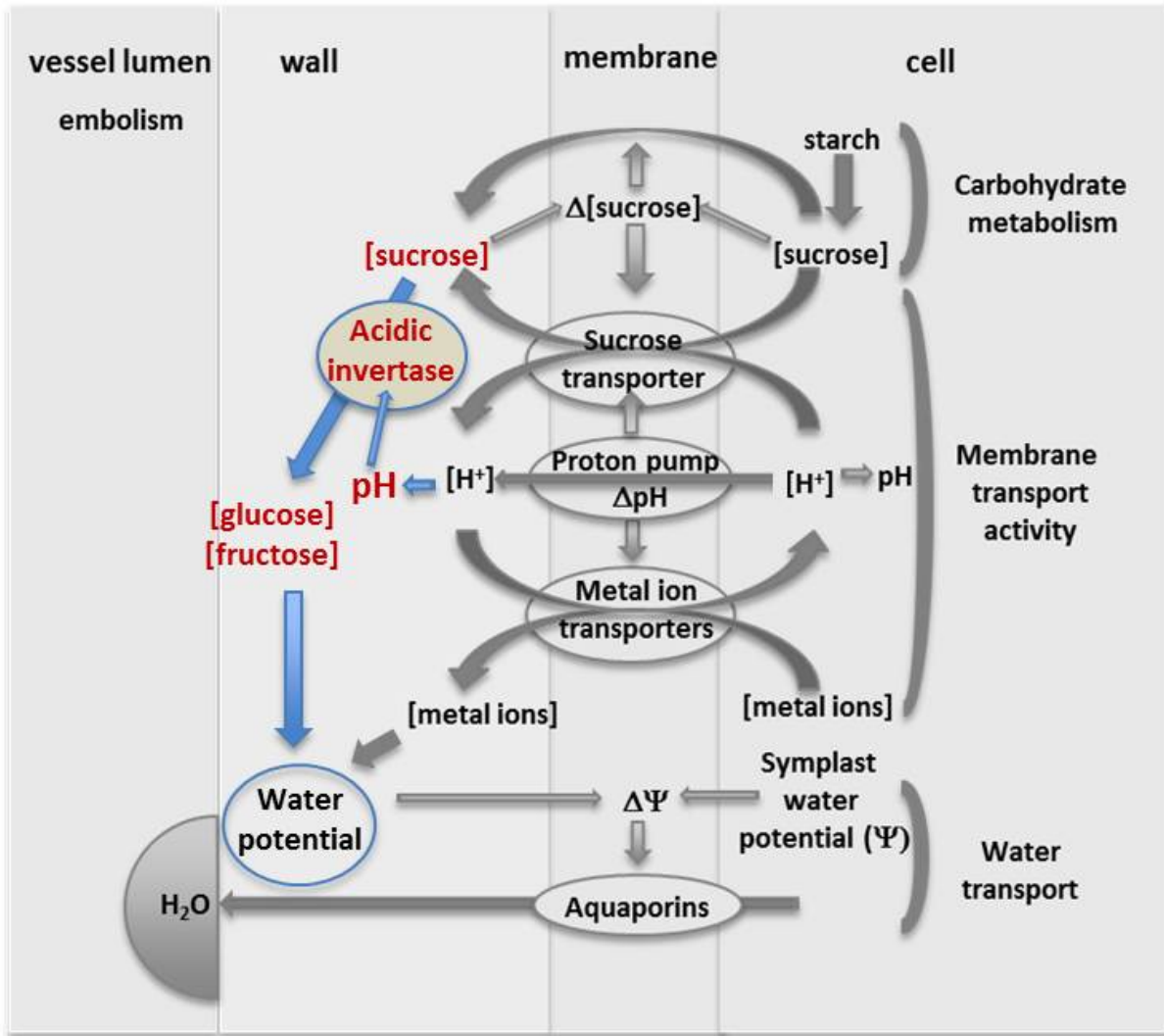
643 **Figure 6**



644

645

646 **Figure 7**  
647



648

649

650